Deformationsüberwachung und Modellierung mit LiDAR-Daten für Beurteilung der Hangstabilität

Deformation monitoring and modeling based on LiDAR data for slope stability assessment

Hui Hu[1], Tomás M. Fernández Steeger[1], Mei Dong[1], Rafig Azzam[1]

[1] M.sc. Hui Hu, Lehrstuhl für Ingenieurgeologie und Hydrogeologie, RWTH Aachen. hu@lih.rwth-aachen.

Zusammenfassung

Lockergesteinssedimente reagieren mit zeitabhängigen Deformationen, wenn sie durch Einschnitte entlastet werden. Diese Zeitabhängigheit stellt eine Herausforderung, wenn es um die stabilitätsbewertung geht. Mit der Ziel eine fortschrittliche Technik zur Bearbeitung und Schadensminderung von Versagensfällen in Lockergestein zu entwickeln, wurde terrestrisches Laserscanning (TLS) verwendet um multitemporale hochauflösende, dreidimensionale Oberflächendaten einer hohen, frisch geschnittenen Tagebauböschung in sandig und tonigem Lockeregestein zu erhalten. Es wurden vier aufeinanderfolgende Scanaufnahmen über einen Zeitraum von drei Monaten hinweg aufgenommen. Anschließend wurde ein Programm erstellt, welches ein auf TLS Daten basierende geologisches Modell in ein geotechnisches Modell für numerische Simulationen transferiert. Dabei werden Methoden wie das maximale Entfernungsverfahren oder die Bestimmung des Ausmaßes von geometrischen Kennzeichen verwendet, um aus den geologischen Modell Böschungsverformungen in mm Auflösung zu erkennen. In einem iterativen Prozess werden durch gerichtete Optimierung die Kombination für die geotechnischen Böschungsparameter ermittelt, welche die beobachteten Verformungen in einem FE-Modell am besten beschreibt. Deformationserkennungen und äquivalente geotechnische Modell tragen zur Beurteilung der Hangstabilität bei.

Schlüsselworte: Deformationsüberwachung, Erkennung von Deformation, LiDAR, numerische Modellienrung, Hangstabilitätanalyse, Rückenanalyse

Abstract

Time dependent deformation is a common process in soil slopes but never the less a challenging task for stability assessment. Slope failure and the land subsidence originating not only from extensive constructions and mining but also due to geological processes are common problems, which adversely influence environment, human safety and economic development. In order to pursue an advanced methodology for management and mitigation of soil slope failure, such points as adequate monitoring technology, effective deformation recognition, reliable numerical modeling, and precise slope stability analysis are important to be taken into account.

Within this scope, a terrestrial laser scanner (TLS) was adopted to collect high resolution point cloud data from a fresh cut high slope in sandy and clayey soils in an open pit mine. Therefore, four scanning campaigns have been conducted over a period of three months. A conversion tool to transfer a LiDAR data-based 3D geological model into a 3D geotechnical model for numerical simulation has been developed. Two sophisticated techniques, i.e. both maximum distance method and feature degree method, were proposed to recognize the slope displacement in mm resolution from the surface model. In an iterative process with numerous numerical forward simulations, presumed geotechnical parameters and resultant movements were investigated to find the suitable solutions of parameter combinations for the FE-model which enable to describe the observed deformation process. This allows to determine the factor of safety for the slopes, as well as a revision of geotechnical parameters, through finite element slope stability analyses combined with automatic strength reduction technique.

Keywords: Deformation monitoring, Deformation detection, LiDAR, Numerical modeling, Slope stability analysis, Back analysis

1 Introduction

Slope failure and the land subsidence originating not only from extensive constructions and mining but also due to geological processes are common problems, which adversely influence environment, human safety and economic development. Time dependent deformation is a common process in soil slopes but never the less a challenging task for stability assessment. The extremely high and steep slope mostly exists in open pit mine due to pursuing the maximum profits and causes unstable slope. The occurrence of a small precursor prior to slope collapse is strong evidence (Hoek and Bray, 1981), which demonstrates most slope failures taking place after enough accumulation of displacements. Glastonbury and Fell (2002) interpreted that combination of developing and warning systems, selectingslope deformation criteria, and designing stabilization or risk mitigation measures is the standard method for dealing with slope instability problem.

Since 1960s, a series of monitoring instruments have been used and developed in open pit mines for periodic or real-time observation. A newly developed LiDAR technology as non-contact monitoring which is capable of observing deformation of complete target and providing high resolution of mm level digital elevation model (HRDEM) has been widely used in various fields. The challenge is how to efficiently analyze the mass LiDAR data, how to recognize the valuable information, and how to make use of it for numerical simulation. Synchronously, development of stability analysis method has consistently been taken into account. Limit equilibrium methods (LEMs) are still most commonly used, but numerical methods are more sophisticated than LEMs. In general, FEM slope stability analyses can be classified into two categories, slip surface stress analysis (SSA) based and strength reduction technique (SRT) coupled. SSA-based FEM represents the combination of LEM and FEM, and FEM coupled with SRT enables to arrive at the threshold of slope failure.

In order to design a workflow which concerns slope stability in surface mine or land subsidence in underground mine, such bullet points as deformation monitoring, deformation detection, FEM modeling and slope stability assessment should be given attention and combined in the framework. Figure 1 shows the kernel of the combination of these bullet points that equivalent geotechnical parameters can be obtained via deformation based back analysis and enable numerical slope stability analysis.

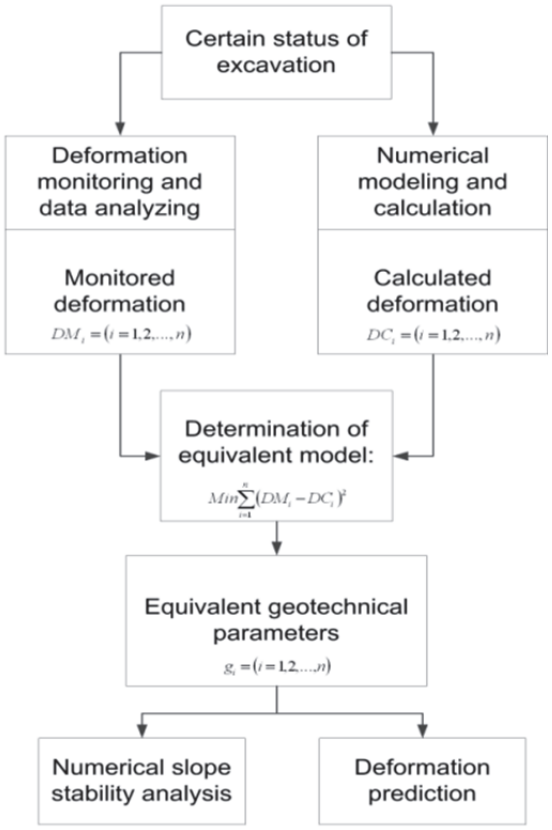

Abb. 1: Equivalent geotechnische Parameter aus Deformation zurück.

Fig. 1: Equivalent geotechnical parameters from deformation based back analysis

2 Study Area and Field Investigation

2.1 Study Area

The present research was cooperation between RWE Power AG and Department of Engineering Geology and Hydrogeology, RWTH Aachen University, which was carried out in open pit mine Hambach, Germany, and dedicates to establishing an available workflow concerning slope monitoring, deformation detection and FEM slope stability analysis.

The open pit mine Hambach (strip mine, in Niederziel and Elsdorf, i.e. the heart of the Rhenish lignite mining area, located in the Lower Rhine Embayment in the triangle formed by the cities of Cologne, Aachen and Duesseldorf, North-Rhine Westphalia, Germany) is the largest one of the RWE for the promotion of lignite open pit mine. Begun in 1978, the mine currently has a size of 39.32 km^2 (measured in early 2011) and is approved to eventually have a size of up to 85 km^2. It is also the deepest open pit mine with respect to sea level, where the ground of the pit is 293 m below sea level. The lignite formations of the Lower Rhine Basin consists of Miocene (main coal measures), Pliocene and Pleistocene deposits. The fresh cutting slope scanned comprises two layers, such as sand and clay.

2.2 Field Investigation

Mining activities are carried out on the deepest stage, i.e. the 7th stage of the whole open pit mine, the scanning station was deployed on the 6th floor, and the target of interest is the slope surface of the 5th stage. In order to monitor the slope deformation in open pit Hambach, the multicampaigns scanning was carried out. Two TLS scanners, i.e. Optech ILRIS-3D and Riegl system, were synchronously used to monitoring, which is shown in Figure 2. The TLS scanning campaign started on 1st April 2011 and was followed by the three campaigns on 13th April, 12th May, and 20th June in the same year. The Trimble GPS system was located on the positions of both scanners and control points to register the scanned target in the geodetic coordinate system. For ILRIS-3D, the multi-scans are required to cover the entire area of interest and the resultant data need to be aligned to a model during data processing.

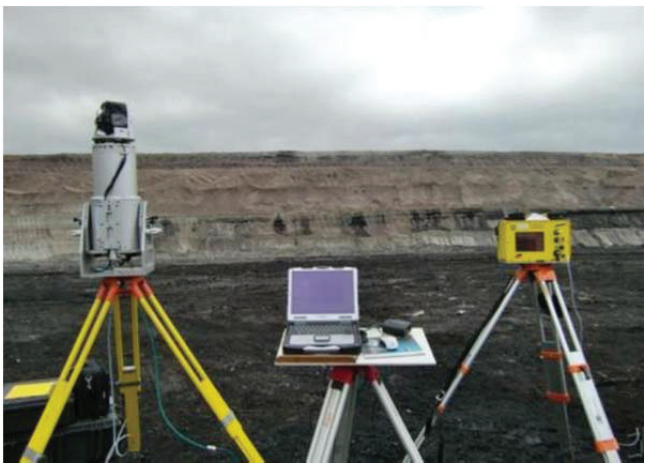

Abb. 2: TLS Bereitstellung für Felduntersuchung.

Fig. 2: TLS deployment for field investigation.

Two scanning positions marked as ScanPos 1 and ScanPos 2 were set up in each scanning campaign. ILRIS 3D scanned three times from left to right at ScanPos 1 and three times from right to left at ScanPos 2 to enhance the resolution of data obtained. On the first scan campaign, four control points were set up, which are mark 4000 and mark 3000 located on the 6th floor close to the toe of the scanned slope, as well as mark 2000 and mark 1000 located on the 5th floor close to the crown of the scanned slope. Because of external interference, only mark 1000 remained in the 2nd campaign, and the others altered the positions. Furthermore, mark 1000 changed its location as well in the 3rd and the 4th campaigns.

The historical terrain documents enable to simplify the excavation process, which is shown in Figure 3. Figure 3 presents that the 6th floor where we set up the TLS was on the same level with the 5th floor. Mining promotion caused the change of the 6th stage. When the excavation on the 6th stage stopped, TLS investigation started (part e of Figure 3). After the second scan campaign, more overburden of the 5th stage was excavated (from part e to part f of Figure 3). Therefore the upper control points altered to farer from the scanner (part g of Figure 3). This simplified excavation process plays an important role in determination of equigeotechnical parameters of overburden material.

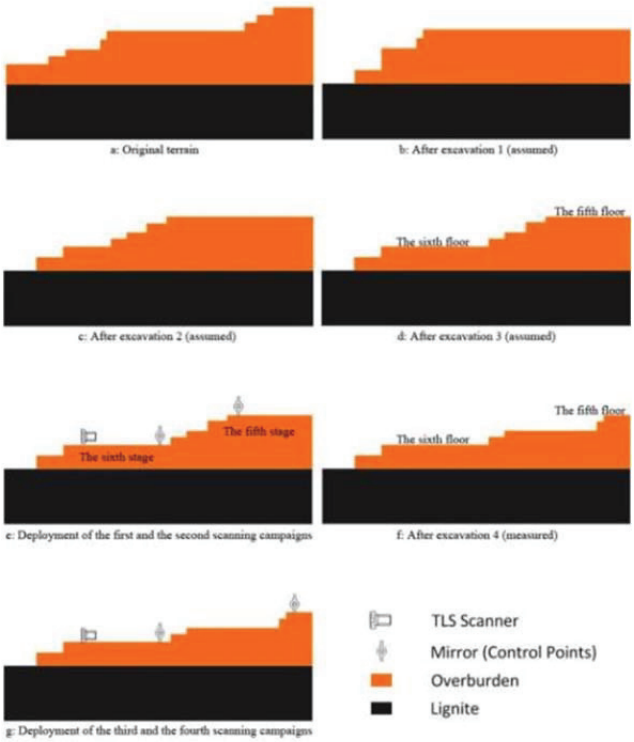

Abb. 3: Prozess von vereinfachten Aushub.

Fig. 3: Sketch of simplified excavation process.

3 Deformation Detection

3.1 State of the art

In the past 20 years, remote sensing (RS) technology has been increasingly applied to monitor landslide and other geo-hazards. Through multi-temporal DTMs derived from airborne LiDAR, the landslide displacements can be tracked in a rough level of meter (Dewitte et al., 2008). Some progresses regarding feature detection have been achieved. Wang and Yuan (2010) made use of curvature and density of point cloud data to detect features. The technique with Gauss map clustering is appropriate for identifying the sharp features (Weber, 2010). These methods are qualified to extract feature points from the objects with regular geometry, e.g. buildings, vehicles, and other real objects which could be mathematically described. However, slope in open pit is in nature with extremely complex topography, and frequently influenced by external dynamic impacts. The most commonly used methods for deformation detection are not capable of detecting and extracting the natural feature points from the multi-temporal HRDEMs.

3.2 Micro-view Deformation Detection

The key in micro-view deformation detection is feature point, which can be differentiated from its neighboring points in an image. To precisely determine whether a point is the feature point, the following two aspects should be satisfied:

- To be a feature point, it must present the prominent characteristic of an object and stands at a summit, a nadir, or a vertex of an irregular shape;
- Besides, a neighborhood of the feature point should serve as a foil to highlight the desirable feature point.

Two new methods, named maximum distance (MD) and feature degree (FD), which can deal with the multi-temporal HRDEMs for deformation detection, are proposed here. The feature detection and extraction are the kernels in both methods. The fundamental preparations for both methods require to select sufficient patches which encompass at least one discernible feature point and illustrated in Hu's Doctoral thesis (2012). The following workflow is the guideline for both MD and FD methods:

- Selection of sufficient patches;
- Structure the data into uniform;
- Construction of neighborhood in which the feature degree of each point will be calculated and visualized (only for FD);
- Calculation of MD or FD;
- Extraction of feature points from the selected patch;
- Recognition of deformation.

3.2.1 Maximum Distance

With respect to a certain 3D object with cone, convex or concave shape, it is feasible to identify at least one point using MD method. Regression plane which is constructed based on all data of a patch determines the uniqueness of feature point. As most selected patches are typically presented as cone, convex, and concave, a hollow-closed 3D object can be constructed by sealing a plane to the data of selected patch. Regression can be performed in Matlab code. Distance of each point to the regression plane can be computed in compliance with general distance. Having a 3D spatial point (x_0, y_0, z_0) in 3D Cartesian coordinate system, a spatial plane can be expressed by:

$$f(x,y,z) = ax + by + cz + d = 0$$

the normal vector of plane is given by:

$$v = \begin{bmatrix} a \\ b \\ c \end{bmatrix}$$

and a vector from the plane to a specific point is given by:

$$w = \begin{bmatrix} x_0 \\ y_0 \\ z_0 \end{bmatrix}$$

Distance D from specific point to plane can then be determined via projection of w to v:

$$D = \frac{vw}{v} = \frac{|ax_0 + by_0 + cz_0 + d|}{\sqrt{a^2 + b^2 + c^2}}$$

Dropping the absolute value signs gives the signed distance:

$$D = \frac{ax_0 + by_0 + cz_0 + d}{\sqrt{a^2 + b^2 + c^2}}$$

which is positive if the vectors w and v are on the same side of the plane. Once the distance of each point to the regression plane are computed, the maximum, minimum and certain configuration distances to the regression plane can be determined, which is shown in Figure 4.

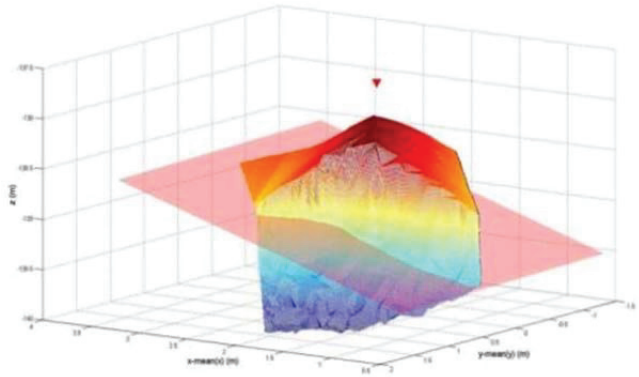

Abb. 4: Wirksamkeit der MD-Methode.

Fig. 4: Effectiveness of MD method.

3.2.2 Feature Degree

Feature degree method consists of four steps: neighborhood definition of each point, determination of normal vector, calculation of feature degree, and extraction of feature points. As data structure is uniformed to grid type, the neighborhood can be defined on the 2D plane x~y, which is shown in Figure 5. For instance, the neighborhood of the point $p_{i,j}$ consists of eight surrounding points in a square form. The surrounding points can be determined by calculation of distance of them to $p_{i,j}$. After having a neighborhood N_p with eight nearest points constructed for $p_{i,j}$ belonging P (point set). Since each point has its own normal vector, each point has its own feature degree. Normal vector is simply called as normal which is perpendicular to a regression plane. FD method calculates the outward-pointing normal vector of each point, and this method is based on regression plane as well. $n_{i,j}$ is defined as the feature degree of point $p_{i,j}$. Eight angle differences of surrounding normal vector to center normal vector can be calculated by:

$$\begin{cases} \emptyset_1 = \emptyset\left(n_{i,j}, n_{i-1,j-1}\right) = \Delta\left(n_{i,j}, n_{i-1,j-1}\right) \\ \vdots \\ \emptyset_8 = \emptyset\left(n_{i,j}, n_{i,j-1}\right) = \Delta\left(n_{i,j}, n_{i,j-1}\right) \end{cases}$$

The sequence of calculation for angle differences is clockwise starting from the lower left corner of one neighborhood. The feature degree $n_{i,j}$ is the arithmetic mean value of the eight angle differences given by:

$$n_{i,j} = \sum_{k=1}^{8} \emptyset_k / 8$$

The extraction of feature points can be referenced in Hu's doctoral thesis (2012). The effectiveness of FD method for extraction of feature points is shown in Figure 6.

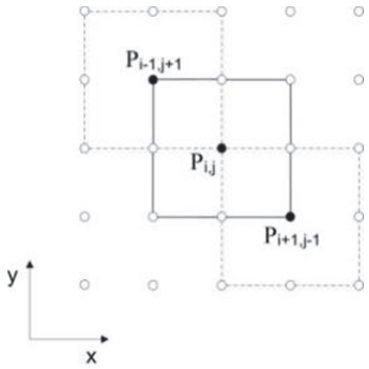

Abb. 5: Grid Datenstruktur und Nachbarschaft des Punktes.

Fig. 5: Grid data structure and neighborhood of point.

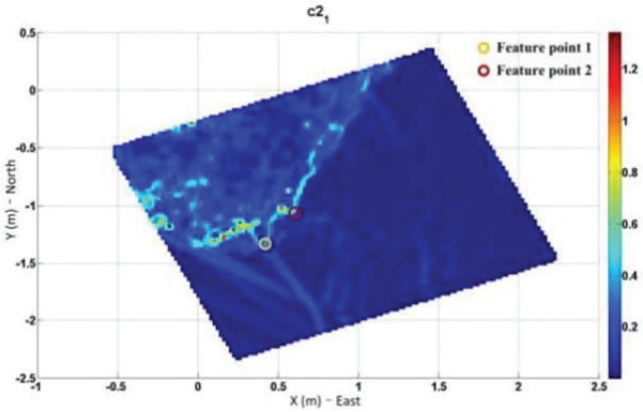

Abb. 6: Wirksamkeit der FD-Methode.

Fig. 6: Effectiveness of FD method.

3.3 Deformation Result

Taking feature point c20 as example, and c20_1 means point c20 of the 1st scan campaign. Deformation result of point c_20 is listed in Table 1. Table 2 lists results of all extracted feature points. The results demonstrate that it is difficult to distinguish the deformation of the scanned slope along x direction and y direction. Three all groups show the expansion from the 1st campaign the 3rd campaign, and the shrink from 3rd to 4th. Expansion phenomenon has an agreement with the influence of unloading due to mine excavation.

Tab. 1: Deformation von Merkmalspunkt c20.
Tab. 1:Deformation result of feature point c20.

Label	Feature degree	D_x (m)	D_x (m)	D_x (m)
C20_1	0.283	0.000	0.000	0.000
C20_2	0.319	0.002	-0.030	0.019
C20_3	0.233	-0.025	-0.014	0.071
C20_4	0.250	0.021	-0.016	0.000

Tab. 2: Deformaion von drei Gruppen entlang dreier Achsen.
Tab. 2:Deformaion of three groups along three axes.

	Direction	1-1 (m)	2-1 (m)	3-1 (m)	4-1 (m)
Group1	x	0.0000	-0.0089	-0.0106	-0.0027
	y	0.0000	-0.0041	-0.0579	-0.0211
	z	0.0000	**0.0636**	**0.1183**	**0.0225**
Group2	x	0.0000	-0.0064	-0.0310	-0.0141
	y	0.0000	0.0238	-0.0399	0.0398
	z	0.0000	**0.072**	**0.1233**	**0.007**
Group	x	0.0000	0.0195	0.0094	0.0295
	y	0.0000	-0.0521	-0.0788	-0.0487
	z	0.0000	**0.0882**	**0.1352**	**0.0204**

4 Equivalent Geotechnical Model

4.1 Mathematical Model

Sakurai (1997) presented a procedure for assessment of the structure stability and design/construction. It can be extended for deformation prediction and slope stability analysis, which is shown in Figure 1. Given the deformation results, the mathematic model to obtaining equivalent geotechnical parameters can be described as follows:

Having the monitored deformation at a series of representative points:

$$DM_i = (i = 1,2, \dots, n)$$

and given the trial of geotechnical parameters:

$$g_i = (i = 1,2, \dots, n)$$

the corresponding deformation calculated by FEM forward analysis is noted as:

$$DC_i = (i = 1,2, \dots, n)$$

The objective function is a minimum sum squared error of the monitored deformation and the calculated deformation:

$$f = min \sum_{i=1}^{n} (DM_i - DC_i)^2$$

4.2 Artificial Neural Network for Back Analysis

4.2.1 Back propagation Neural Network (BPNN)

BPNN is a multi-layer dynamic system optimization neural network. BPNN workflow achieves the objective function which is shown in Figure 7. In general, BPNN consists of three layers (input layer, hidden layer, and output layer), each of which has neurons.

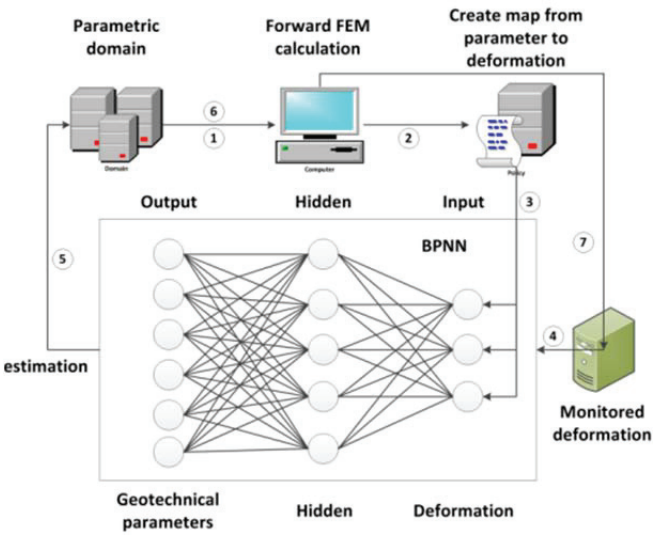

Abb. 7: Deformationsrückanalyse durch BPNN.
Fig. 7: Deformation back analysis based on BPNN.

Figure 7 shows 5 milestones described below:

Samples preparation: orthogonal design and normalization of geotechnical parameters within parametric domain need to be implemented, and the map from parameters to deformation need to be created via forward FEM calculation. It is represented in step 1 and 2.

Configuration of neural network: set up the number of hidden layer (as 1), the number of hidden neuron (as 4), and the number of input (as 3) and output (as 2) neuron which is subject to the number of displacement observation nodes and parameters to be inversed. In this case, 3 inputs are the detected deformations of three groups, and 2 outputs are the unloading modulus E_u of clay and sand layers of the slope.

Training and testing: calculated deformation is deemed as input, and corresponding geotechnical parameter as target. The big proportion of samples is used to training a net, while the rest of them to testing the net. It is identical with step 3.

Determination of parameters: monitored deformation is input to the net trained to determine the geotechnical parameters (outputs). It is accomplished by step 4, 5, 6, and 7. The quality of outputs needs to be estimated through a iteration process which runs from step 3 to step 7.

4.2.2 Training and Testing

BPNN training and testing were performed in a developed Matlab Neural Network Tool (MNNT). Correlation between targets (geotechnical parameters of sample) and outputs (geotechnical parameters calculated via net) enables to show the quality of net obtained. Figure 8 discloses the correlation coefficient between targets and outputs of training samples, which is 0.98794. Figure 9 reveals the correlation coefficient of 0.94191 between targets and outputs of testing samples. It is demonstrated that the net has qualified to predict the unloading modulus E_u.

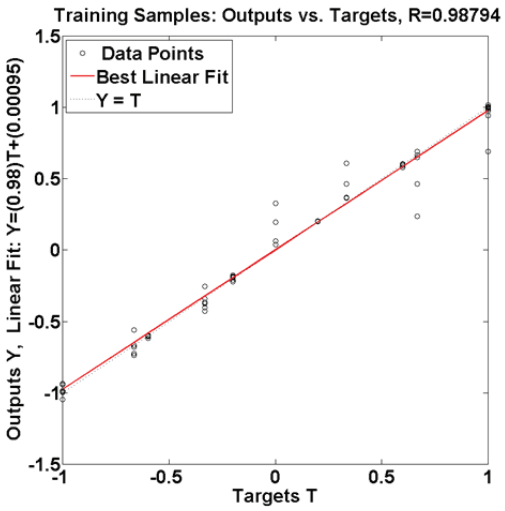

Abb. 8: Korrelation zwischen den Zielen und Ausgänge von Lernstichprobe.

Fig. 8:Correlation between targets and outputs of training sample.

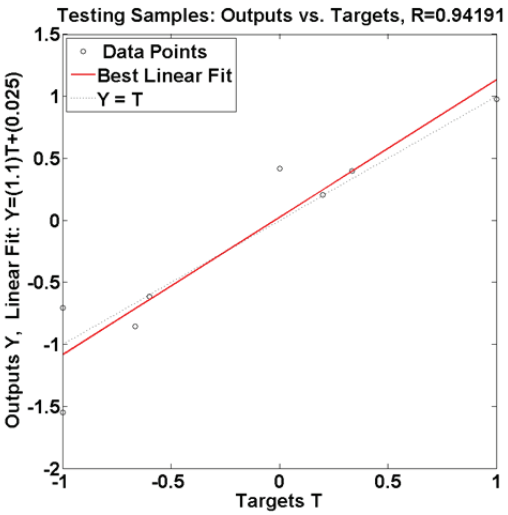

Abb. 9: Korrelation zwischen den Zielen und Ausgänge von Teststichprobe.

Fig. 9:Correlation between targets and outputs of testing sample.

4.3 Equivalent Geotechnical Parameters

Geotechnical parameters which can be easily ascertained by empirical approaches or experiments are fixed prior to determination of E_u. Equivalent geotechnical parameters (Table 3) make FEM forward simulation more agreed with deformation monitored. To verify the reliability of E_u, the calculated deformation based on the fixed parameters should be compared with the detected deformation. The maximum discrepancy of both is 3.33% (Table 4), which discloses that the equivalent geotechnical parameters are adequate for FEM assessment of slope stability.

5 Conclusion

Multi-campaigns HRDEMs derived from LiDAR technology enable to achieve effective deformation detection in *mm* level. To do so, maximum distance and feature degree methods were proposed to recognize and extract the feature points, so called deformation detection, which represent the motion of a complete slope scanned. On basis of the concept of equivalent geotechnical model, back propagation neural networks was applied into determination of some geotechnical parameters difficult to be ascertained. Verification through comparing detected deformation and calculated deformation qualifies equivalent geotechnical model for FEM assessment of slope stability. The factor of safety (FOS) of the slope can be determined through FEM simulation coupled with automatic strength reduction technique, and the reliability of determined FOS can be improved by time series analysis which requires periodical TLS scanning campaign.

Tab. 4: Vergleich der berechnete und entdeckt Deformation.

Tab. 4:Comparison of calculated and detected deformation.

	Clay	Sand
Density (kg/m3)	2268	2125
Eu (Mpa)	96	80
Poisson's ratio	0.4	0.3
Friction angle (°)	25	35
Cohesion (Pa)	60000	10

Tab. 4: Vergleich der berechnete und entdeckt Deformation.

Tab. 4:Comparison of calculated and detected deformation.

	t1	t2	t3
Detected deformation (cm)	10.83	12.33	13.52
Calculated doformation (cm)	10.81	12.74	13.97
Discrepancy (%)	-0.81	3.33	3.33

Literatur

HOEK, E. & BRAY, J. (1981): Rock Slope Engineering, Taylor & Francis. 2.

GLASTONBURY, J. & FELL, R. (2002): A Decision Analysis Framework for Assessing Post-failure Velocity of Natural Rock Slopes, University of New South Wales.

HU, H. (2012): Deformation Monitoring and Modeling based on LiDAR Data for Slope Stability Assessment, Doctoral Thesis Submitted, RWTH Aachen University.

DEWITTE, O., JASSELETTE, J., CORNET, Y., VAN DEN EECKHAUT, M., COLLIGNON, A., POESEN, J., DEMOULIN, A. (2008): Tracking landslide displacements by multi-temporal DTMs: A combined aerial stereophotogrammetric and LIDAR approach in western Belgium, Engineering Geology, 99: 11-22.

WANG, L. & YUAN, B. (2010): Curvature and Density based Feature Point Detection for Point Cloud Data, IET 3rd International Conference on Wirless, Mobile and Multimedia Networks.

WEBER, C., HAHMANN, S., HAGEN, H. (2010): Sharp Feature Detection in Point Clouds, IEEE International Conference on Shape Modeling and Applications (SMI) 2010, S: 1-12.

SAKURAI, S. (1997): Lessons learned from _eld measurements in tunnelling, Tunnelling and Underground Space Technology, 12: 453-460.